TẠP CHÍ KHOA HỌC
TRƯỜNG ĐẠI HỌC QUY NHƠN

Đánh giá về việc sử dụng các tính toán hóa học lượng tử trong phát triển các cảm biến huỳnh quang

Nguyễn Khoa Hiền[1], Phan Thị Diễm Trân[1,2], Mai Văn Bảy[3], Phạm Cẩm Nam[4], và Dương Tuấn Quang[2,*]

[1]Viện Nghiên cứu Khoa học Miền Trung, Bảo tàng Thiên nhiên Việt Nam, Viện Hàn lâm Khoa học và Công nghệ Việt Nam,Việt Nam
[2]Trường Đại học Sư phạm, Đại học Huế, Việt Nam
[3]Trường Đại học Sư phạm, Đại học Đà Nẵng, Việt Nam
[4]Trường Đại học Bách Khoa, Đại học Đà Nẵng, Việt Nam

Ngày nhận bài: 18/02/2022; Ngày sửa bài: 24/10/2022;
Ngày nhận đăng: 28/10/2022; Ngày xuất bản: 28/10/2022

TÓM TẮT

Trong bài đánh giá này, các ứng dụng tính toán hóa học lượng tử được công bố gần đây trong việc phát triển cảm biến huỳnh quang đã được giới thiệu, bao gồm các tính toán trong quá trình phát triển cảm biến huỳnh quang mới dựa trên sự chuyển electron do cảm ứng ánh sáng (PET); nghiên cứu cấu trúc, tính chất và bản chất của các tương tác trong các hợp chất, đặc điểm hấp thụ và huỳnh quang của các hợp chất dựa trên các tính toán của trạng thái cơ bản và trạng thái kích thích, và phân tích obitan liên kết thích hợp (NBO). Các ứng dụng này có thể không toàn diện, nhưng chúng nhằm mục đích làm nổi bật, hướng dẫn và thúc đẩy việc sử dụng các tính toán hóa học lượng tử cho quá trình phát triển các cảm biến huỳnh quang.

Từ khóa: *Tính toán hóa học lượng tử, cảm biến huỳnh quang, PET, trạng thái cơ bản, trạng thái kích thích.*

**Tác giả liên hệ chính.*
Email: dtquang@hueuni.edu.vn

https://doi.org/10.52111/qnjs.2022.16502

QUY NHON UNIVERSITY
JOURNAL OF SCIENCE

On the use of quantum chemical calculations in the development of fluorescent sensors

Nguyen Khoa Hien[1], Phan Thi Diem Tran[1,2], Mai Van Bay[3], Pham Cam Nam[4], and Duong Tuan Quang[2,*]

[1]Mientrung Institute for Scientific Research, Vietnam National Museum of Nature, Vietnam Academy of Science and Technology, Hue, Vietnam
[2]Department of Chemistry, University of Education, Hue University, Vietnam
[3]The University of Danang, University of Science and Education, Vietnam
[4]The University of Danang, University of Science and Technology, Vietnam

Received: 18/02/2022; Revised: 24/10/2022;
Accepted: 28/10/2022; Published: 28/10/2022

ABSTRACT

In this review, recently published quantum chemical computing applications in the development of fluorescent sensors were introduced, including the calculations in the development of the photoinduced electron transfer (PET) - based new fluorescent sensors; the study of structure, property, and nature of interactions, absorption, and fluorescence characteristics of compounds based on calculations of the ground state and excited state, and the natural bond orbital (NBO) analysis. These applications may not be comprehensive, but they aim to highlight, guide and promote the use of quantum chemical computation in the development of fluorescent sensors.

Keywords: *Quantum chemical calculations, fluorescent sensors, PET, ground state, excited state.*

1. INTRODUCTION

Today, along with the development of computer science, from hardware to software, simulation methods and theoretical computation are strongly developed and becoming effective tools in many fields, especially in chemistry,[1] physics,[2] biology,[3,4] medicine,[5,6] and environmental issues[7].

The Nobel Prize in Chemistry 2013 was awarded to the work "the development of multiscale models for complex chemical systems" by Martin Karplus (Université de Strasbourg, France and Harvard University, Cambridge, MA, USA), Michael Levitt (Stanford University School of Medicine, Stanford, CA, USA), and Arieh Warshel (University of Southern California, Los Angeles, CA, USA), implemented since 1970. Before those studies, the Nobel Prize in Chemistry 1995 was awarded to three computational chemists, Paul J. Crutzen, Mario J. Molina, and F. Sherwood Rowland for their work in atmospheric chemistry, particularly concerning the formation and decomposition of ozone. The Nobel Prize in Chemistry 1998 was divided equally between Walter Kohn for his development of the density-functional theory and John A. Pople for his development of computational methods in quantum chemistry. These are considered as a vivid evidence, honoring the effective contributions of computational chemistry.

**Corresponding author.*
Email: dtquang@hueuni.edu.vn

https://doi.org/10.52111/qnjs.2022.16502

Up to now, computational chemistry has been successfully applied in various fields. In particular, computational chemistry is widely used in studying the structural characteristics, the nature of bonds and the properties of compounds;[8,9] the ability to participate in reactions, pathways, mechanisms and products of chemical reactions.[10,11] On that basis, computational chemistry has been flexibly applied in many different fields.

In materials research, computational chemistry is used to study the structure,[12] material properties such as ionization energy, binding energy, HOMO and LUMO energy gap,[12] UV-Vis spectra, the catalytic role of metal clusters,[13] the relationship between structure with inhibition of metal corrosion, and metal corrosion remedies.[14,15]

In drug research, computer-aided drug design (CADD) is a computational chemical method that effectively assists in screening and evaluating the biological activity of active ingredients such as inhibitory activity on cancer cells,[16] inhibitory activity on virus and enzymes,[17-19] antioxidant properties, free radicals scavenging activities.[20] This method helps to screen, evaluate and quickly detect active ingredients with desired activity in tens of thousands of research compounds.[21] This helps to reduce significantly the volume of experimental research, shorten the research time, as well as clarify the nature and mechanism of the processes.[22] Therefore, there are many publications on Covid-19 treatment drugs using this method.[23,24]

The main content of this review focuses on introducing recently published quantum chemical computing applications in the development of new fluorescent sensors. These applications may not be comprehensive, but they aim to highlight, guide and promote the use of quantum chemical computation to the development of fluorescent sensors.

2. RESULTS AND DISCUSSION

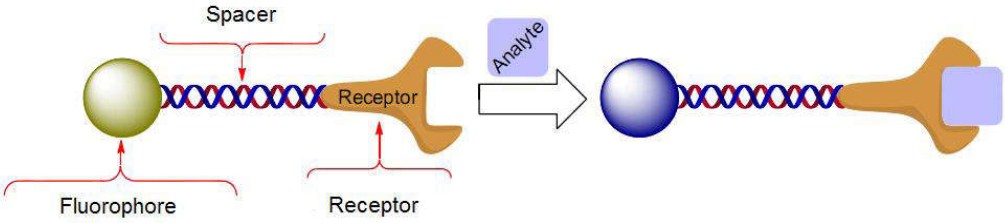

Figure 1. Basic compositions of a fluorescent sensor.[25]

The fluorescent sensors are molecular sensors based on the change of fluorescence signal resulting from the interaction of the analytes with sensors. The fluorescent sensor is typically composed of three main parts: "fluorophore–spacer–receptor" (Figure 1).[25] Figure 2 shows an illustration of a fluorescent sensor with three main parts for detection of HClO in cancer cells.[26]

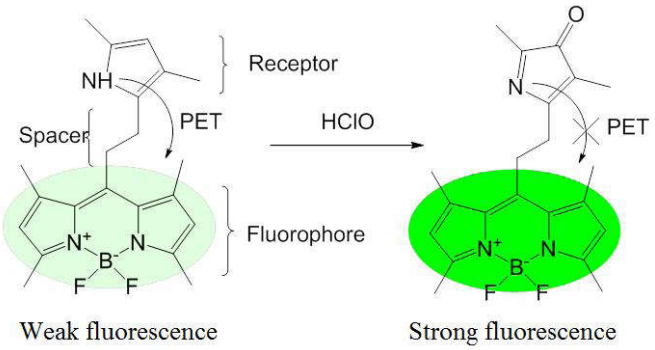

Figure 2. An illustration of fluorescent sensor with three main parts "fluorophore-spacer-receptor".[26]

The first fluorescent sensor is a chemodosimeter based on spirolactam ring-opening process of rhodamine B derivative for the detection of Cu(II) ions, published in 1992 by A. W. Czarnik.[26] Nowadays, the number of published new fluorescent sensors has been rapidly increased. New fluorescent sensors have been reported almost every week in the world.[27] This is because the fluorescent sensors are often sensitive to the analytes, easy to carry out, and less expensive.[28] In particular, fluorescent sensors can be used for detection of some items in living cells like Fe(III) in Hepatic cells,[29] Cu(II) in HepG2 cells,[30] Hg(II) in PC3 cells[31]…

Following the successes of computational chemistry, new computer-aided-developed fluorescent sensors have been published more and more regularly. This is because these processes have made the development of new fluorescent sensors more efficient. In which, quantum chemistry calculations have been orienting experimental research, helping to reduce the volume of experimental studies, increase the probability of success, as well as clarify the nature and mechanism of processes, create a scientific basis for further research.

a) Quantum chemistry calculations in the development of PET (Photoinduced Electron Transfer) - based fluorescent sensors

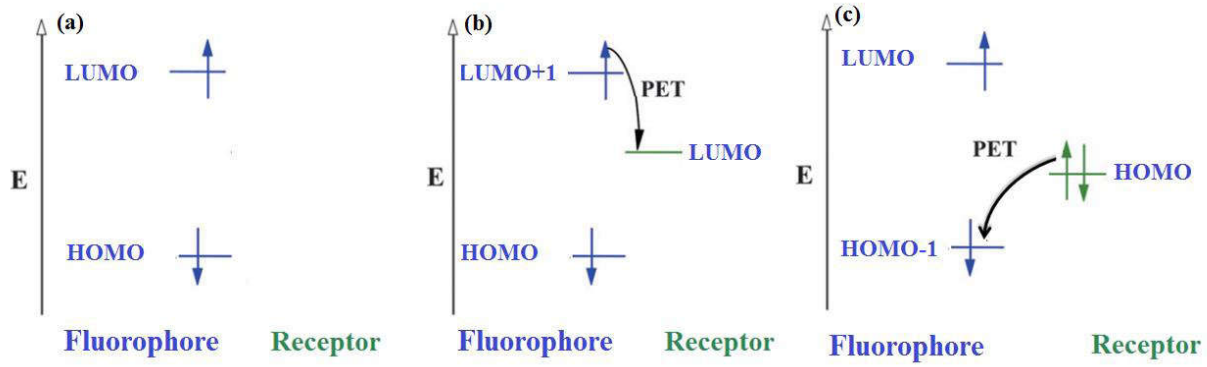

Figure 3. Electron transition process in excited state of fluorescent sensor without PET process (a), with PET process (b), (c).[32,33]

Computational chemistry has been used to study fluorescent sensors which operate based on PET mechanism, mainly the calculations for selection of the appropriate fluorophores and receptors, or for explaination of fluorescent signal changes.[32,33] For fluorescent sensor without PET process, the transition of electron from ground state to excited state takes place in two consecutive MOs (of the fluorophore), LUMO and HOMO (Figure 3a).[32,33] In this case, the de-excitation process is the transition of electron from LUMO to HOMO, and is accompanied by fluorescence emission. Meanwhile, for fluorescent sensor with PET process, the transition of electron from ground to excited state takes place in two non-consecutive MOs (of the flurophore). There is an empty orbital (Figure 3b) or a filled orbital (Figure3c) (of receptor) whose energy level lies between the two orbitals of the transition of electron from ground state to excited state. In this case, the de-excitation process occurs the PET process, which is the transition of electron from LUMO+1 to LUMO (Figure 3b), or from HOMO to HOMO-1 (Figure 3c). This leads to the de-excitation process without fluorescence emission. The reaction between PET sensors and the analytes induces either the presence or the absence of orbital whose energy level lies between the two orbitals in the main transition of the fluorophore, resulting in fluorescence quenching or enhancement, respectively.[32,33]

https://doi.org/10.52111/qnjs.2022.16502

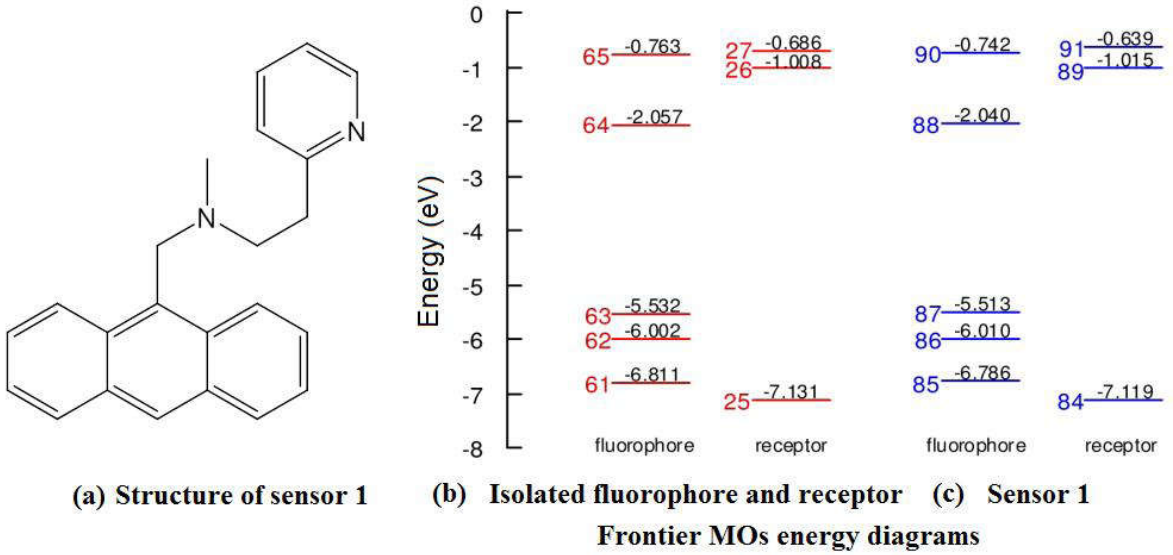

Figure 4. Structure of sensor (a), Frontier MOs energy diagrams of isolated fluorophore and receptor (b), and of sensor **1** (c)[34]

When designing sensor **1** for detection of Zn(II) ion based on anthracene derivative as a fluorophore and pyridine derivative as a receptor, George A. Hudson and co-authors used the density functional theory (DFT)/B3LYP and time-dependent (TD)-DFT/B3LYP methods, with the basis set 6-31G(d,p), 6-31+G(d,p), 6-311G(d,p), and 6-311+G(d,p) to calculate the relative energy levels of the frontier MOs of compounds. The calculation results showed that the relative energy levels of the frontier MOs of compounds were not nearly unchanged when using the above six basis sets. This indicated that any of the above six basis sets can be used in calculating the relative energy levels of the frontier MOs.

The calculation results also showed that the relative energy levels of the frontier MOs of the independent fluorophore and receptor were not nearly altered when they were linked together in sensors (Figure 4). Therefore, it was possible to select fluorophores and receptors for the design of sensors based on the calculation results of the frontier MOs energy levels in the isolated parts. These are promising outcomes for the computational design of sensors.[34]

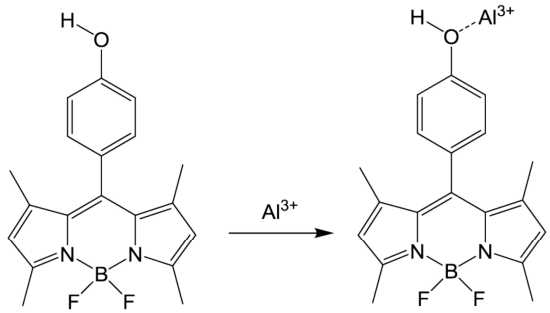

2

Figure 5. Fluorescent sensor **2** for detection of Al(III) based on BODIPY derivative.[35]

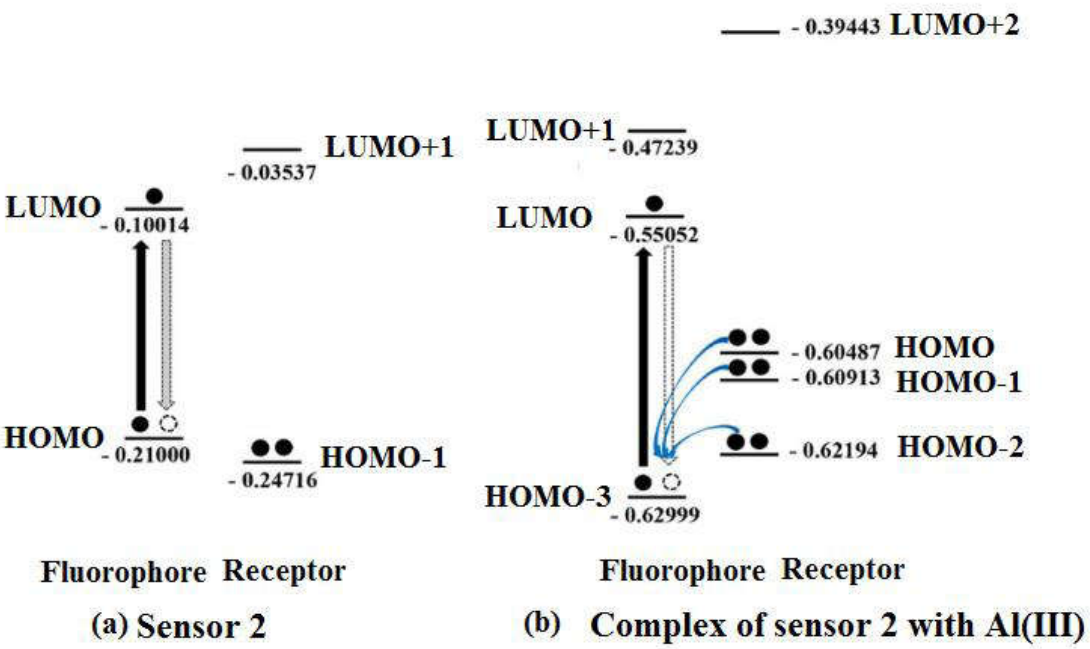

Figure 6. Frontier MOs energy diagrams of sensor **2** (a), complex of sensor **2** with Al(III) (b).[35]

Fluorescent sensor **2** for detection of Al(III) based on BODIPY (boron-dipyrromethene) derivative was published by Tasawan Keawwangchai and co-authors (Figure 5). In this work, the authors used TD-DFT method to explain the experimental results of the change in fluorescent signal before and after the sensor **2** reacted and formed complex with Al(III). In the free state of sensor **2**, the singlet electron transition from the ground state to the excited state was mainly contributed by the HOMO→ LUMO transition. Therefore, the PET process does not occur in sensor **2** and it is a fluorescent compound (Figure 6a). Meanwhile, in the complex of sensor **2** with Al(III), the singlet electron transition from the ground state to the excited state was mainly contributed by the HOMO-3→ LUMO transition (Figure 6b). This leads to the occurrence of PET process and the complex does not emit fluorescence.[35]

In general, on the basis of the operating mechanism of the PET fluorescent sensor, the theoretical calculations have been successfully used in determining the relative energy levels of the frontier MOs of the fluorophore and receptor to design sensors, investigating on the electron transition in excited state to predict or explain the fluorescence properties of compounds.[34-39] The calculated results predicting the fluorescence properties of the compounds were in good agreement with the experimental results.[36-38,39-40] However, this approach may face some limitations. It is only possible to confirm that a compound does not fluoresce when the PET process is determined.[39] In contrast, although the PET process was not found in a compound, it could not be confirmed that it was a fluorescent compound. It is due to many other reasons, for example, the HOMO and LUMO energy gap is too small,[41] the lack of overlapping between HOMO and LUMO.[41,43] In these cases, further study to excited states is essential.

b) Study of the structure, absorption and fluorescence characteristics of compounds based on the calculations of the ground state (GS) and excited states (ESs)

As another application, computational chemistry has been used to study the structure, absorption and fluorescence characteristics of fluorescent sensors and compounds, by using calculations of the GS and Ess.[44-57]

Shigehiro Sumiya and co-authors introduced fluorescent sensor **3** for detection of Hg(II) (Figure 7). In this work, the absorption and fluorescence properties of compounds were studied by using DFT and TD-DFT method to calculate the excitation processes based on their optimized geometries at the (GS). The calculation results in Table 1 show that in sensor **3**, the $S_0 \rightarrow S_2$ transition is the most dominant of the singlet electronic transitions from GS to ESs, with an oscillator strength (*f*) of 0.290, much stronger than that of the other transitions. The $S_0 \rightarrow S_2$ transition is mainly contributed by HOMO→LUMO transition, with a largest contribution of 72.27%. The corresponding excitation energy is 2.91 eV (427 nm).[44]

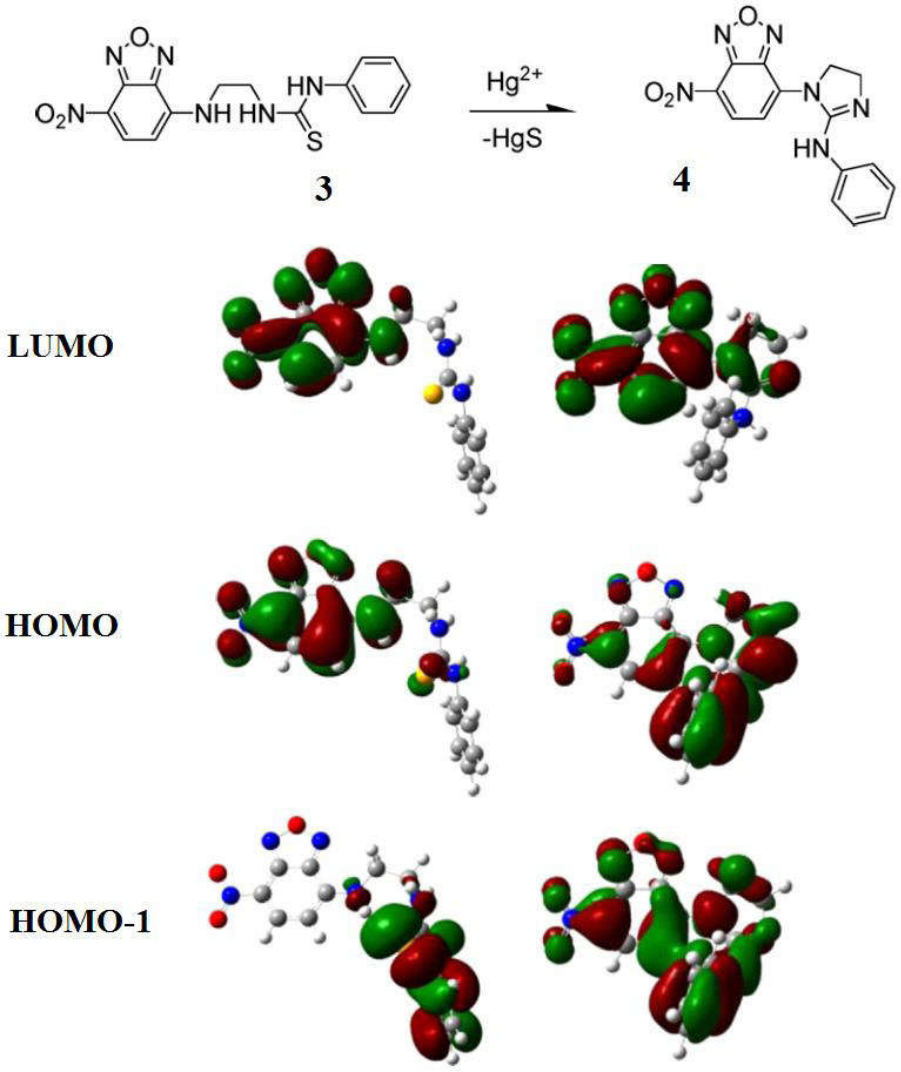

Figure 7. Sensor **3** and frontier MOs of sensor **3** and compound **4.**[44]

For compound **4**, the $S_0 \rightarrow S_2$ transition is also the most dominant of the singlet electronic transitions from GS to ESs, with a greatest oscillator strength (*f*) of 0.333. This transition is mainly contributed by HOMO-1→LUMO transition, with a largest contribution of 75.04%. The corresponding excitation energy is 2.80 eV (443 nm).[44] This calculation results are found be in good agreement with the experimental maximum absorption wavelengths of **3** and **4**, 468 nm and 462 nm, respectively.[44] In sensor **3**, the singlet electron transition from GS to ES takes place in two consecutive MOs (HOMO → LUMO), resulting in no PET process. Meanwhile, in compound **4**, the singlet electron transition from GS to ES takes place in two non-consecutive

MOs (HOMO-1 → LUMO), resulting in PET process.[44] The calculation results of frontier MOs of compounds (Figure 7) also show that, in sensor **3**, the electron density in HOMO and LUMO is predominantly distributed on the NBD moiety. Meanwhile, the electron density in HOMO-1 is predominantly distributed on aniline moiety. Therefore, the PET process from aniline to NBD subunits in the excited state does not occur and sensor **3** is a fluorescent compound. In compound **4**, the electron density in HOMO-1 and LUMO is predominantly distributed on the NBD moiety, the electron density in HOMO is predominantly distributed on aniline moiety. Therefore, the PET process from aniline to NBD subunits in the excited state occurs, and **4** is not a fluorescent compound.[44]

Table 1. Calculated excitation energy (E), wavelength (λ), and oscillator strength (f) for low-laying singlet state of sensor **3** and compound **4**.[44]

Compound	Main transitions		*E*(eV)	*λ*(nm)	*f*	Percentage contribution (%)
3	$S_0 \rightarrow S_1$	HOMO-2→LUMO	2.86	433.2	0.0059	8.64
		HOMO-1→LUMO				88.31
	$S_0 \rightarrow S_2$	HOMO-1→LUMO	2.91	426.7	0.2906	3.19
		HOMO→LUMO				72.27
		HOMO→LUMO+1				5.09
4	$S_0 \rightarrow S_1$	HOMO-1→LUMO	2.34	530.4	0.0397	10.13
		HOMO→LUMO				86.37
	$S_0 \rightarrow S_2$	HOMO-1→LUMO	2.80	442.8	0.3337	75.04
		HOMO→LUMO				5.35

The research results showed that there was a good agreement between the experimental and calculated absorption spectra.[39-44,58] However, it is necessary to select methods, functions and basis sets for the research objects to obtain good results.

For example, there were different methods used to calculate excited states such as TD-DFT, BSE@GW, CIS, CIS(D), ADC(2), CC2, ADC(3), EOM-CCSD, CC3, EOM-CCSDT, SCI, FCI, EOMCCSDTQ, and CASPT2/NEVPT2 methods. Denis Jacquemin and co-authors performed a comparative evaluation of these methods.[59] Each method had its own advantages and limitations. Currently, the TD-DFT method is most commonly used because it is simple, suitable for large molecules,[60] contains many functions, so it can be improved by editing, or adding or subtracting functions.[61]

Duong Tuan Quang and co-authors used the PBE, BP86, PBE0, B3LYP, M06, M06-2X, CAM-B3LYP, LC-wPBE, APDF, wB97XD and PW6B9D3 functions to calculate the maximum absorption wavelength of 21 coumarin derivatives. The results showed that M06-2X functional gave the best predictive performance, with the smallest value of the mean absolute error (MAEfix = 7 nm).[62]

In summary, each method, function or basis set has its own advantages and limitations. They are usually only suitable for specific research purposes and objects. Therefore, it is necessary to evaluate when using, or verifying based on experimental data.

Theoretical investigations on the excitation processes based on optimized ground state geometry (GS) are mainly used to investigate singlet electron transitions from GS to excited

https://doi.org/10.52111/qnjs.2022.16502

states (ESs), thereby predicting or explaining the absorption and fluorescence properties based on excitation process. This method does not directly study the singlet electron transitions from ES to GS. Therefore, the nature of the fluorescence emission process is not clarified, the fluorescence emission wavelength cannot be determined exactly. This is only solved when calculations on optimized geometries of excited states (ESs) are used to directly study the singlet electron transitions from ESs to GS.[48]

Figure 8 shows the Jablonski diagram for calculation of excitation energy and fluorescence emission energy in a simple case. Accordingly, the vertical absorption energy ($E^{vert\text{-}abso}$) from GS to ES is the difference between the energy of ES and GS at the ground state optimized geometry (R^{GS}). The vertical fluorescence energy ($E^{vert\text{-}flu}$) from ES to GS is the difference between the energy of ES and GS at the excited state optimized geometry (R^{ES}).[49,50]

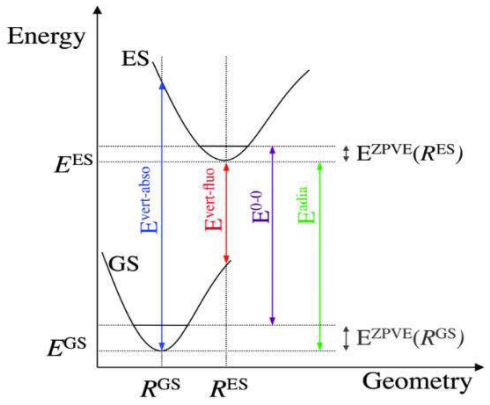

Figure 8. Jablonski diagram for calculation of excitation energy and fluorescence emission energy.[49,50]

Nguyen Khoa Hien and co-authors introduced fluorescent sensor **5** for detection of biothiols (Figure 9). The results of the theoretical investigations on the electron excited states by TD-DFT method show that the fluorescence of the product of the addition reaction between sensor **5** and biothiols is not in accordance with Kasha's rule. This is an exception from the Kasha's rule. Fluorescence emission occurs from the higher lying singlet electron excited state (S_2) instead of the lowest lying singlet electron excited state (S_1). This is because the electron transition from S_1 to S_0 is forbidden since the lack of overlapping between MOs in transition, and the small energy gap between S_2 and S_1 excited states. The fluorescence from the higher-lying singlet electron excited states leads to markable fluorescence enhancement at long wavelength in the products of addition reaction between biothiols and sensor **5**.[43]

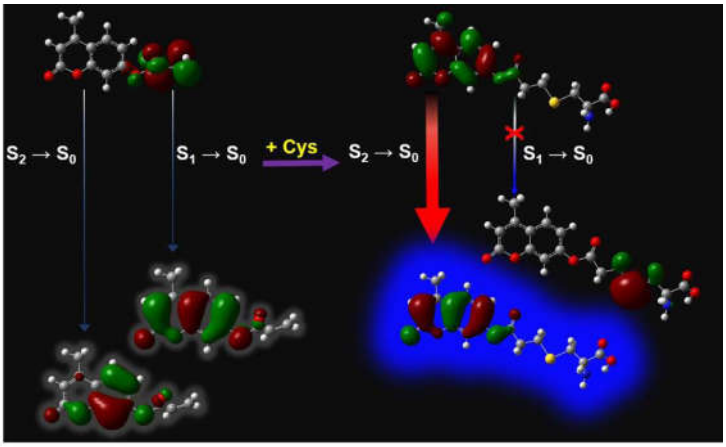

Figure 9. Sensor **5** for detection of bithiols based on coumarin derivative.[43]

Caterina Bernini and co-authors investigated the excited state geometries and emission energies of 11 organic D-π-A dyes, with using the CAM-B3LYP, MPW1K, ωB97X-D, LC-BLYP, LC-ωPBE, and M06-HF functionals, in combination with the cc-pVDZ, 6-31+G(d,p), and 6-311+G(2d,p) basis sets. Polarizable Continuum Model was also performed in both LR and SS formalisms. The LR-PCM/TD-DFT results showed that accurate emission energies were obtained only when solvent effects and a range separated hybrid functional was used. The maximum mean absolute error of the vertical emission energy was 0.2 eV. The accuracy was further improved using the SS-PCM formalism.[56] According to this approach, some publications have successfully applied to investigate on the absorption and fluorescence spectra of compounds, as evidenced by a quite good agreement between theoretical calculations and experimental results.[51-55] However, calculation on optimized geometry of excited states is not simple. This requires an extremely strong configuration of computer system rather than calculations on optimized geometry of ground state, especially for large compounds, complexes and in the environment of solvents. Therefore, up to now, the calculations on excited state optimized geometry are still very rarely published, and mainly used for small and simple compounds.[51-55]

In addition, theoretical investigations on excitation processes are also applied to study the mechanisms of some other processes, such as the excited state intramolecular proton transfer (ESIPT),[56] twisted intramolecular charge transfer (TICT)[57]...

Yang Li and Tian-Shu Chu used DFT and TD-DFT methods to study the excitation processes of fluorescent compound **6** (Figure 10). The calculated results on the optimized geometry and energy of the ground state and excited states show that there is an ESIPT process. Accordingly, compound **6** exists as an enol in its ground state. In the excited state, it converts to compound **7** in the keto form through an ESIPT process, resulting in a shift in fluorescence emission to the long wavelength region.[56]

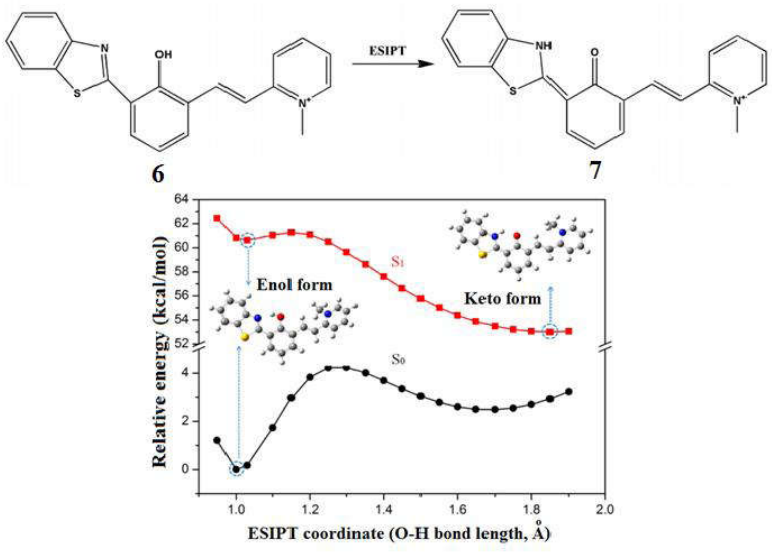

Figure 10. Theoretical investigation of an ESIPT case in fluorescent compound **6**.[56]

When utilizing DFT and TD-DFT methods to study the fluorescence properties of 4-N, N-dimethylamino cinnamaldehyde (**8**), Surajit Ghosh and co-authors reported that, after being excited, compound **8** undergone the twisted intermolecular transformation to reach a minimum on the potential energy surface (PES), accompanied by twisted intramolecular charge transfer (TICT), resulting in a transition from locally excited (LE) state to TICT excited state

https://doi.org/10.52111/qnjs.2022.16502

(Figure 11). Due to the intramolecular charge transfer, the polarization of the TICT state was higher than that of the LE state. As a result, the TICT state was more stable than the LE state in solvents of greater polarity. This led to a red shift in fluorescence emission and absorption, from weaker polar solvents to stronger polar solvents.[57]

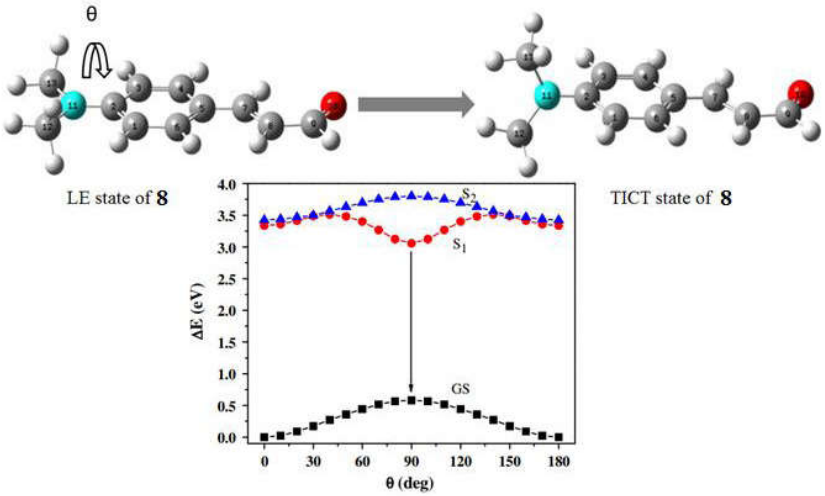

Figure 11. Theoretical investigation of an TICT case in fluorescent compound **8**.[57]

Mai Van Bay and co-authors introduced fluorescent sensor **9** for detection of Hg(II) ions (Figure 12).[43] The DFT calculation results show that **9** molecule is composed of three moieties, in which ethylenediamine as a spacer is the bridge between rhodamine and dimethylamino-cinnamaldehyde (DACA). Rhodamine moiety in **9** exists in the spirolactam ring form and is not a fluorescent compound. Although the configuration of the DACA moiety in **9** is unchanged from the free state of DACA fluorophore, **9** is a non-fluorescent compound. This has been clarified when studying excitation states. TD-DFT calculation results show that after being excited, the molecule **9** undergoes intramolecular twisting, accompanied by the process of the twisted intermediate charge transfer (TICT). As a result, there is a transition from the locally excited (LE) state to the TICT excited state. Consequently, the $S_1 \rightarrow S_0$ de-excitation occurs at TICT state. Unfortunately, the strong charge transfer in the TICT state leads to a complete difference in the localization of electron density, resulting in the lack of overlapping between HOMO and LUMO. The $S_1 \rightarrow S_0$ transition at TICT state is strongly forbidden. These may be the reasons why RLED does not fluoresce.[43]

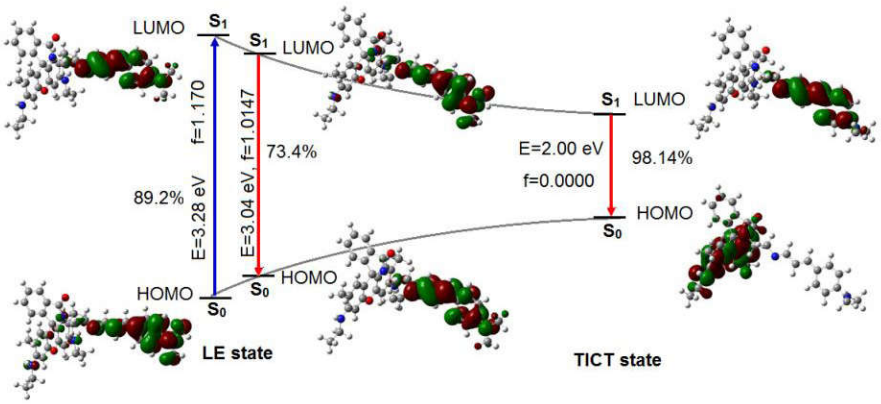

Figure 12. TD-DFT calculations used to explain the fluorescence properties of **9**.[43]

c) Study of the structure, property and nature of interactions in compounds, absorption and fluorescence characteristics of compounds based on the natural bond orbital (NBO) analysis

When studying fluorescent sensors, a fairly common application of computational chemistry is the use of NBO analysis to investigate the structure, property and nature of interactions in compounds. The calculation results obtained from NBO analysis are mainly second-order interaction energy and charges of atoms in molecules. The second-order interaction in NBO analysis is the interaction between the NBO donor and NBO acceptor. The greater second-order interaction energy leads to the stronger interaction, the more stable bond, and the greater degree of conjugation in the system. Therefore, NBO analysis is often used to investigate the degree of conjugation of the π electron system, thereby explaining the fluorescence properties, as well as comparing the durability of compounds based on the value of the second-order interaction energy.[63-65]

When studying a fluorescent sensor for detection of Fe(III) based on 4-(2-hydroxybenzylideneamino) benzoic acid (**10**), Gurpreet Singh and co-authors computed NBO analysis to study the fluorescence properties of compounds. The calculation results showed that there existed a π electron conjugation system in the molecule of sensor **10**. That caused sensor **10** to be fluorescent (Figure 13).[63]

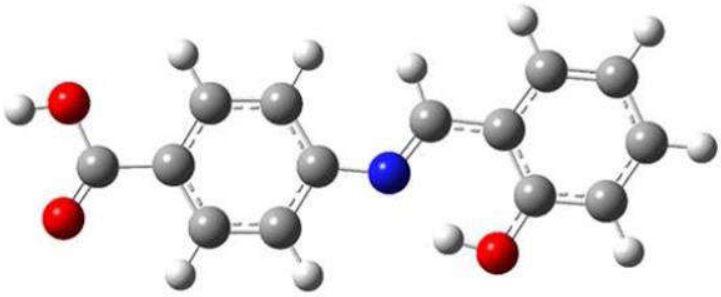

10

Figure 13. Fluorescent sensor **10** for detection of Fe(III).[63]

When studying fluorescent sensor **11** used for detection of Cu(II) and Hg(II) (Figure 14), Yong Xia and co-authors conducted NBO analysis to investigate on the interactions in complexes between sensor **11** with metal ions including Cu(II), Hg(II), Zn(II), Cd(II), and Pb(II). The calculation results showed that the complexes were stabilized mainly by donor-acceptor interactions from lone pair (LP) of the O and N atoms to the empty LP* or RY* (Rydberg) orbitals of the central metal ions. In this case, the interactions from the LP of the N atoms to the LP* or the RY* of the metal ions were much stronger than the interactions from the LP of the O atoms. The calculation results also showed that these interactions in Hg(II) complex were stronger than those in Cu(II) complex, and even stronger than in other complexes. As a result, the most stability was Hg(II) complex, followed by the Cu(II) complex, and then the other complexes. These results were completely consistent with the calculation results in which the Gibbs free energy of complexation reaction of **11** with Hg(II), Cu(II), Zn(II), Cd(II), and Pb(II) was -433.3, 386.9, 333.6, 276.7, and 236.6 kcal.mol^{-1}, respectively. These results led to the prediction that Hg(II) may react to displace Cu(II) from the complex between Cu(II) and sensor **11**. Therefore, sensor **11** could also be used to detect Hg(II).[64]

https://doi.org/10.52111/qnjs.2022.16502

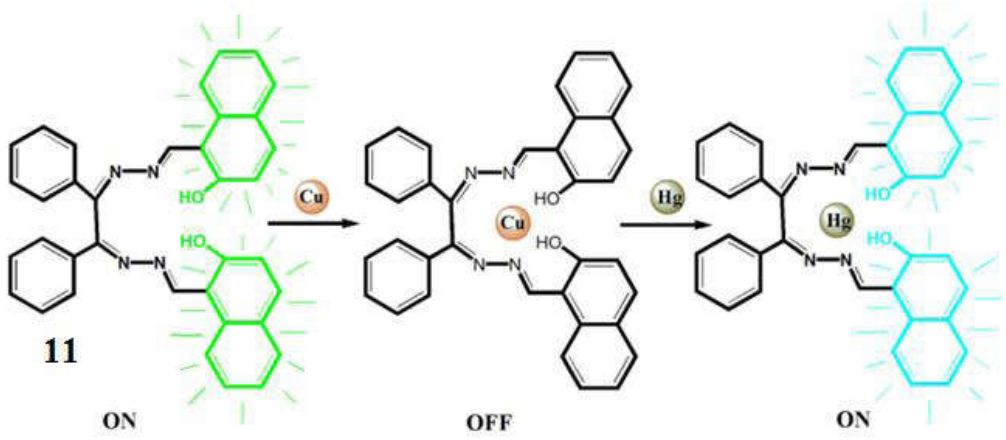

Figure 14. Fluorescent sensor **11** for detection of Cu(II) and Hg(II).[64]

A fluorescent sensor (**12**) based on benzothiazolium hemicyanine derivative for Hg(II) detection was synthesized and studied by Doan Thanh Nhan and co-authors (Figure 15).[41] Free sensor **12** exhibited a red emission at 585 nm. Hg(II) coordinated to ligand **12** with a stoichiometry of 1:1 and led to the fluorescence quenching. The detection limits of the colorimetric and fluorescent method are 15.3 and 11.8 ppb, respectively. The optimized molecular structures, absorption and fluorescence characteristics of the sensor L and its complex with mercury ions were carried out using the calculations at the B3LYP/LanL2DZ level of theory, combined with Atoms In Molecules and Natural Bond Orbitals analyses. The NBO analysis results showed that the complex was stabilized mainly by donor-acceptor interactions from lone pair (LP) of the O and S atoms to the empty LP* orbitals of the central mercury atom. The formation of these interactions led to a significant transfer of electron density from ligands to the metal ions, and broke the π-electron conjugated system in the **12** ligands. This was an important factor leading to fluorescence quenching and color change in the complex.

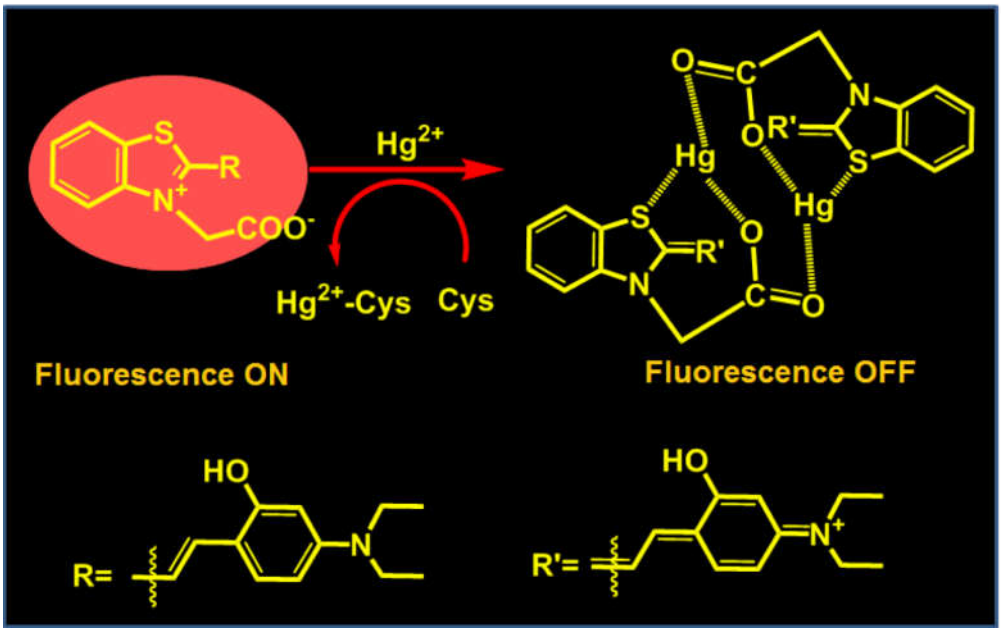

Figure 15. Fluorescent sensor **12** for detection of Hg(II) based on benzothiazolium hemicyanine derivative.[41]

d) Determine values of energy and constants for reactions based on the optimized geometries and the single point energies of the compounds

Sairam S Mallajosyula and co-authors used computational chemistry to study the mechanism of action of a 1,3-dithiole-2-thione-based fluorescent sensor (**13**) (Figure 16). The optimized geometric structures of sensor **13** and its complexes with metals and water were carried out using the DFT method and the B3LYP/LanL2DZ level of theory. From these structures, the authors calculated the formation energy of complexes and determined the pathway of complex exchange reaction between $As(H_2O)_3$ and ligand P (sensor **13**). The calculation results also showed that the formation of AsP_3 complex was more thermodynamically favorable than that of HgP_4 complex, with more negative formation energy of -174.19 kcal.mol^{-1}. Since then, sensor **13** was predicted to be more selective detection of As(III), compared with Hg(II).[65]

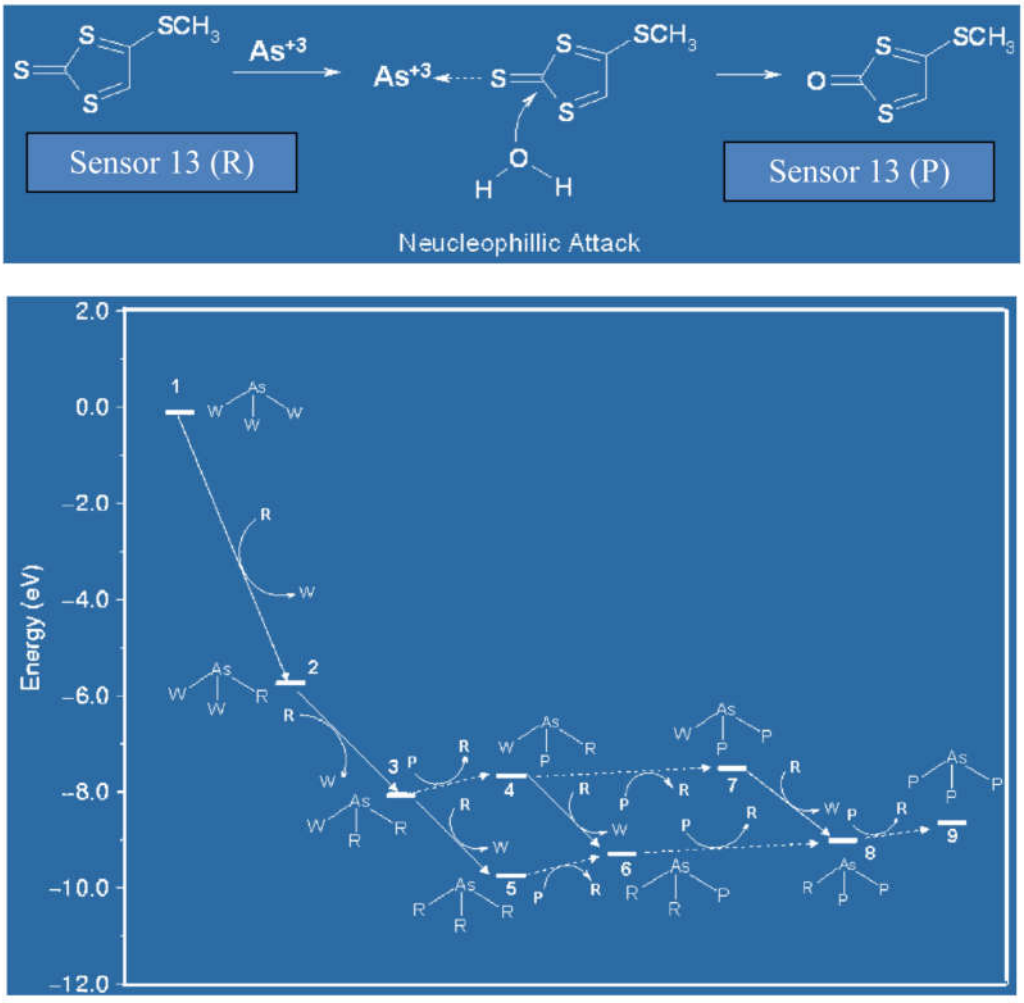

Figure 16. Theoretical investigation on mechanism of action of fluorescent sensor **13** (W: H_2O, R: reactant, P: product).[65]

To investigate the possibility of using the complex between **14** and Cu(II) as a fluorescent chemosensor for detection of biothiols (Figure 17a), Nguyen Khoa Hien and co-authors used the theoretical calculations of the stability constant of complex.[58] Accordingly, the theoretical stability constant of the complex was theoretically calculated based on the solvation model and the Gibbs free energy of ligand-exchange reactions, obtained from the thermodynamic cycle (Figure 17a). As a result, the calculated complexation equilibrium constant of 14-Cu(II) was 10^7.[16]

https://doi.org/10.52111/qnjs.2022.16502

This value of complexation equilibrium constant of Cu(II) ions with **14**, was much smaller than of Cu(II) ions with biothiols. These results led to an expectation that the complex of **14** with Cu(II) ions could be used as a fluorescent sensor for detection of biothiols based on the complex exchange reactions. The obtained results were in good agreement with the experimental data. The **14**-Cu(II) complex could be used as a fluorescent sensor for detecting biothiols in the presence of non-thiols containing amino acids, with a detection limit for cysteine of 0.3 µM.[58]

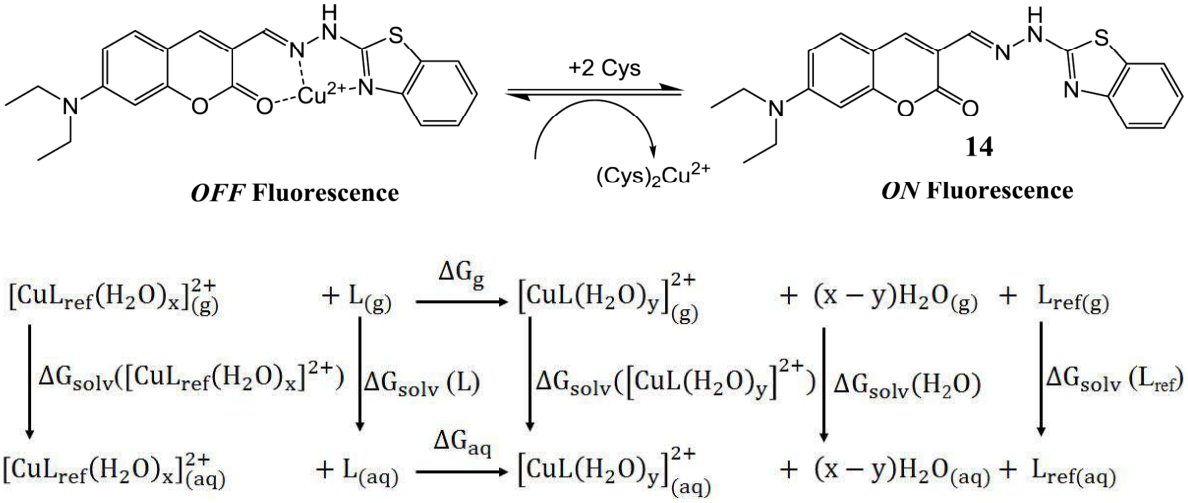

Figure 17. (a) Illustrative diagram of the reaction between the **14**-Cu(II) complex and Cys; (b) Thermodynamic cycle for the calculation of Gibbs free energy of ligand-exchange reaction in aqueous solution, ΔGaq.[58]

3. CONCLUSIONS

This review introduced the recently published quantum chemical computing applications in the development of PET-based fluorescent sensors. It was involved in the study of the structure, absorption, and fluorescence characteristics of compounds based on the calculations of the ground and excited states; the study of the structure, property, and nature of interactions in compounds, absorption and fluorescence characteristics of compounds based on the NBO analysis; and determination of energies and constants for reactions based on the optimized geometries and the single point energies of the compounds.

The results showed that quantum chemical calculations have been successfully used in the design and development of new fluorescence sensors, predicting as well as explaining the absorption and fluorescence properties of compounds. The calculated results are more significant when combined with experimental studies. This combination is to increase the likelihood of success, reduce the volume of experimental study, and create the scientific basis to adjust and recommend appropriate calculation methods for next studies.

REFERENCES

1. E. G. Lewars. *Computational chemistry. Introduction to the theory and applications of molecular and quantum mechanics*, Third edition, Springer, 2016.
2. P. O. J. Scherer. *Computational physics. Simulation of classical and quantum systems*, Third edition, Graduate Texts in Physics, Springer, 2017.
3. R. Wunschiers. *Computational Biology,* First edition, Springer-Verlag, New York, LLC, 2004.
4. S. Shankar, T. Dunning, R. Muller, G. H. Chen (Editors). *Computational materials, chemistry, and biochemistry: From bold initiatives to the last mile. In honor of William A. Goddard's contributions to science and engineering*, Springer Series in Materials Science, Springer, 2020.

5. Nguyen Minh Tam, Minh Quan Pham, Huy Truong Nguyen, Nam Dao Hong, Nguyen Khoa Hien, Duong Tuan Quang, Huong Thi Thu Phung and Son Tung Ngo. Potential inhibitors for SARS-CoV-2 Mpro from marine compounds, *RSC Advances*, **2021**, *11*, 22206-22213.

6. L. Gorb, V. Kuz'min, E. Muratov (Editors). *Application of Computational Techniques in Pharmacy and Medicine (Challenges and Advances in Computational Chemistry and Physics 17)*, Springer, 2014.

7. M. F. Acevedo. *Simulation of ecological and environmental models*, CRC PRESS, 2017.

8. N. Kerru, L. Gummidi, S. V. H. S. Bhaskaruni, S. N. Maddila, P. Singh and S. B. Jonnalagadda. A comparison between observed and DFT calculations on structure of 5-(4-chlorophenyl)-2-amino-1,3,4-thiadiazole, *Scientific Reports*, **2019**, *9*(1), 19280.

9. S. Mirdoraghi, F. Piri and M. Vahedpour. A computational study on multiple formaldehyde complexes and their possible chemical reactions as well as the catalytic effect in the gas phase, *SN Applied Sciences,* **2020**, *2*, 623.

10. C. A. Grambow, L. Pattanaik and W. H. Green. Reactants, products, and transition states of elementary chemical reactions based on quantum chemistry, *Scientific Data*, **2020**, *7*, 137.

11. S. Liu, Y. Wu, C. Zhou, J. Wu and Y. Zhang. Study on the CO formation mechanism during coal ambient temperature oxidation, *Energies*, **2020**, *13*(10), 2587.

12. R. Hussain, M. Saeed, M. Y. Mehboob, S. U. Khan, M. U. Khan, M. Adnan, M. Ahmed, J. Iqbal and K. Ayub. Density functional theory study of palladium cluster adsorption on a graphene support, *RSC Advances*, **2020**, *10*(35), 20595-20607.

13. A. Dutta, P. Mondal. Density functional approach toward the adsorption of molecular hydrogen as well as the formation of metal hydride on bare and activated Carbon-supported rhodium clusters, *Journal of Physical Chemistry C,* **2018**, *122*(29), 16925–16939.

14. V. Chauhan, A. C. Reber and S. N. Khanna. Strong lowering of ionization energy of metallic clusters by organic ligands without changing shell filling, *Nature Communications*, **2018**, *9*, 2357.

15. Duy Quang Dao, Truong Dinh Hieu, Thong Le Minh Pham, Dinh Tuan, Pham Cam Nam, I. B. Obot. DFT study of the interactions between thiophene-based corrosion inhibitors and an Fe_4 cluster. *Journal of Molecular Modeling*, **2017**, *23*(9), 260.

16. H. L. Abdulrahman, A. Uzairu & S. Uba. Computer modeling of some anti-breast cancer compounds, *Structure Chemistry*, **2021**, *32*, 679–687.

17. S. Rampogu, D. Ravinder, S. C. Pawar, and K. W. Lee. Natural compound modulates the cervical cancer microenvironment-A pharmacophore guided molecular modelling approaches, *Journal of Clinical Medicine*, **2018**, *7*(12), 551.

18. K. Klimenko. *Computer-aided drug design of broad-spectrum antiviral compounds*, Université de Strasbourg, 2017.

19. Z. Jin, X. Du, Y. Xu et al. Structure of Mpro from SARS-CoV-2 and discovery of its inhibitors, *Nature*, **2020**, *582*, 289–293.

20. Mai Van Bay, Pham Cam Nam, Duong Tuan Quang, Adam Mechler, Nguyen Khoa Hien, Nguyen Thi Hoa, and Quan Van Vo. Theoretical study on the antioxidant activity of natural depsidones, *ACS Omega*, **2020**, *5*(14), 7895–7902.

21. Son Tung Ngo, Ngoc Quynh Anh Pham, Ly Thi Le, Duc-Hung Pham, and Van V. Vu. Computational determination of potential inhibitors of SARS CoV-2 main protease, *Journal of Chemical Information and Modeling*, **2020**, *60*(12), 5771-5780.

22. M. Hariono, D. B. E. Wijaya, T. Chandra, N. Frederick, A. B. Putri, E. Herawati, L.i A. Warastika, M. Permatasari, A. D. A. Putri, and S. Ardyantoro. A decade of Indonesian atmosphere in computer-aided drug design, *Journal of Chemical Information and Modeling*, **2021**, (DOI: 10.1021/acs.jcim.1c00607).

https://doi.org/10.52111/qnjs.2022.16502

23. Bui Thi Phuong Thuy, Tran Thi Ai My, Nguyen Thi Thanh Hai, Le Trung Hieu, Tran Thai Hoa, Huynh Thi Phuong Loan, Nguyen Thanh Triet, Tran Thi Van Anh, Phan Tu Quy, Pham Van Tat, Nguyen Van Hue, Duong Tuan Quang. Investigation into SARS-CoV-2 resistance of compounds in garlic essential oil, *ACS Omega*, **2020**, *5*(14), 8312-8320.

24. D. Gopal, S. Skariyachan. Recent Perspectives on COVID-19 and computer-aided virtual screening of natural compounds for the development of therapeutic agents towards SARS-CoV-2, *In: Methods in Pharmacology and Toxicology*, Springer, New York, 2020.

25. A. P. D. Silva, T. S. Moody and G. D. Wright. A fluorescent chemodosimeter based on rhodamine derivative for detection of Hg(II) ions studied by using the density functional theory, *Analyst*, **2009**, *134*, 2385–2393.

26. H. Zhu, J. Fan, J. Wang, H. Mu, and X. J. Peng. An "Enhanced PET" - based fluorescent probe with ultrasensitivity for imaging basal and elesclomol-induced HClO in cancer cells, *Journal of the American Chemical Society*, **2014**, *136*(37), 12820–12823.

27. M. Y. Chae and A. W. Czarnik. Fluorometric chemodosimetry. Mercury(II) and silver(I) indication in water via enhanced fluorescence signaling, *Journal of the American Chemical Society*, **1992**, *114*(24), 9704-9705.

28. Duong Tuan Quang and Jong Seung Kim. Fluoro- and chromogenic chemodosimeters for heavy metal ion detection in solution and biospecimens, *Chemical Reviews*, **2010**, *110*(10), 6280-6310.

29. M. H. Lee, T. V. Giap, S. H. Kim, Y. H. Lee, C. Kang, J. S. Kim. A novel strategy to selectively detect Fe(iii) in aqueous media driven by hydrolysis of a rhodamine 6GSchiff base, *Chemical Communications*, **2010**, *46*, 1407-1409.

30. H. S. Jung, J. H. Han, Y. Habata, C. Kang and J. S. Kim. An iminocoumarin–Cu(ii) ensemble-based chemodosimeter toward thiols, *Chemical Communications*, **2011**, *47*, 5142–5144.

31. M. Kumar, N. Kumar, V. Bhalla, H. Singh, P. R. Sharma, and T. Kaur. Naphthalimide appended rhodamine derivative: Through bond energy transfer for sensing of Hg2+ Ions, *Organic Letter*, **2011**, *13(6)*, 1422-1425.

32. B. Valeur. *Molecular fluorescence*: *Principles and applications,* Wiley-VCH: Weinheim – New York – Chichester – Brisbane – Singapore – Toronto, 2001.

33. Y. Yang, Q. Zhao, W. Feng, and F. Li. Luminescent chemodosimeters for bioimaging. *Chemical Reviews*, **2013**, *113*, 192-270.

34. G. A. Hudson, L. Cheng, J. Yu, Y. Yan, D. J. Dyer, M. E. McCarroll, and L. Wang. Computational studies on response and binding selectivity of fluorescence sensors, *Journal of Physical Chemistry B*, **2010**, *114*(2), 870-876.

35. T. Keawwangchai, N. Morakot, B. Wanno. Fluorescent sensors based on BODIPY derivatives for aluminium ion recognition: an experimental and theoretical study, *Journal of Molecular Modeling,* **2013**, *19*, 1435-1444.

36. F. Han, L. Chi, X. Liang, S. Ji, S. Liu, F. Zhou, Y. Wu, K. Han, J. Zhao, T. D. James. 3,6-disubstituted carbazole-based bisboronic acids with unusual fluorescence transduction as enantioselective fluorescent chemosensors for tartaric acid, *Journal of Organic Chemistry*, **2009**, *74*, 1333–1336.

37. X. Zhang, L. Chi, S. Ji, Y. Wu, P. Song, K. Han, H. Guo, T. D. James, J. Zhao. Rational design of d-PeT Phenylethynylated-Carbazole monoboronic acid fluorescent sensors for the selective detection of α-Hydroxyl Carboxylic acids and monosaccharides, *Journal of the American Chemical Society*, **2009**, *131*, 17452-17463.

38. S. Ji, J. Yang, Q. Yang, S. Liu, M. Chen, J. Zhao. Tuning the intramolecular charge transfer of alkynylpyrenes: Effect on photophysical properties and its application in design of OFF–ON fluorescent thiol probes, *Journal of Organic Chemistry*, **2009**, *74*, 4855-4865.

39. Nguyen Khoa Hien, Phan Tu Quy, Nguyen Tien Trung, Vo Vien, Dang Van Khanh, Nguyen Thi

Ai Nhung and Duong Tuan Quang. A dansyl-diethylenetriamine-thiourea conjugate as a fluorescent chemodosimete for Hg2+ ions in water media, *Chemistry Letters*, **2014**, *43*, 1034-1036.

40. Nguyen Khoa Hien, Nguyen Chi Bao, Nguyen Thi Ai Nhung, Nguyen Tien Trung, Pham Cam Nam, Tran Duong, Jong Seung Kim, and Duong Tuan Quang. A highly sensitive fluorescent chemosensor for simultaneous determination of Ag(I), Hg(II), and Cu(II) ions: Design, synthesis, characterization and application, *Dyes and Pigments*, **2015**, *116*, 89-96.

41. Doan Thanh Nhan, Nguyen Chi Bao, Nguyen Thi Ai Nhung, Dinh Quy Huong, Vo Vien, Nguyen Tien Trung, Nguyen Duc Cuong, Nguyen Khoa Hien and Duong Tuan Quang. A Benzothiazolium-derived colorimetric and fluorescent chemosensor for detection of Hg2+ ions, *Chemistry Letters*, **2017**, *46*(1), 135-138.

42. Nguyen Khoa Hien, Doan Thanh Nhan, Won Young Kim, Mai Van Bay, Pham Cam Nam, Dang Ung Van, In-Taek Lim, Jong Seung Kim, Duong Tuan Quang. Exceptional case of Kasha's rule: Emission from higher-lying singlet electron excited states into ground states in coumarin-based biothiol sensing, *Dyes and Pigments*, **2018**, *152*, 118-126.

43. Mai Van Bay, Nguyen Khoa Hien, Subin Son, Nguyen Duy Trinh, Nguyen Tien Trung, Pham Cam Nam, Jong Seung Kim, and Duong Tuan Quang. Hg2+-promoted spirolactam hydrolysis reaction: a design strategy for the highly selective sensing of Hg2+ over other metal ions in aqueous media, *Sensors*, **2019**, *19*(1), 128.

44. S. Sumiya, T. Sugii, Y. Shiraishi, T. Hirai. A benzoxadiazole–thiourea conjugate as a fluorescent chemodosimeter for Hg(II) in aqueous media, *Journal of Photochemistry Photobiology A: Chemistry,* **2011**, *219*(1), 154-158.

45. T. Keawwangchai, B. Wanno, N. Morakot, S. Keawwangchai. Optical chemosensors for Cu(II) ion based on BODIPY derivatives: an experimental and theoretical study, *Journal of Molecular Modeling*, **2013**, *19*(10), 4239-4249.

46. V. Ruangpornvisuti. A DFT study of molecular structures and tautomerizations of 2-benzoylpyridine semicarbazone and picolinaldehyde N-oxide thiosemicarbazone and their complexations with Ni(II), Cu(II), and Zn(II), *Structural Chemistry*, **2007**, *18*(6), 977-984.

47. H. F. Wang, S. P. Wu. Highly selective fluorescent sensors for mercury(II) ions and their applications in living cell imaging, *Tetrahedron*, **2013**, *69*(8), 1965-1969.

48. I. Ljubić and A. Sabljić. CASSCF/CASPT2 and TD-DFT study of valence and rydberg electronic transitions in fluorene, carbazole, dibenzofuran, and dibenzothiophene, *Journal of Physical Chemistry A*, **2011**, *115*(18), 4840-4850.

49. D. Jacquemin, A. Planchat, C. Adamo, and B. Mennucci. TD-DFT assessment of functionals for optical 0–0 transitions in solvated dyes, *Journal of Chemical Theory and Computation*, **2012**, *8*(7), 2359-2372.

50. C. A. Denis. The calculations of excited-state properties with time-dependent density functional theory, *Chemical Society Reviews*, **2013**, *42*, 845-856.

51. R. Carrasquilla and O. N. Bueno. Time dependent density functional study of the absorption and emission spectra of 1,3-benzoxazole and three substituted benzoxazoles, *Optica Pura y Aplicada*, **2012**, *45*(3), 287-297.

52. C. Bernini, L. Zani, M. Calamante, G. Reginato, A. Mordini, M. Taddei, R. Basosi, and A. Sinicropi. Excited state geometries and vertical emission energies of solvated dyes for DSSC: A PCM/TD-DFT benchmark study, *Journal of Chemical Theory and Computation*, **2014**, *10(9)*, 3925-3933.

53. R. Chidthong, S. Hannongbua, A. J.A. Aquino, P. Wolschann, H. Lischka. Excited state properties, fluorescence energies, and lifetime of a poly(fluorene-pyridine) copolymer, based on TD-DFT investigation, *Journal of Computational Chemistry*, **2007**, *28*, 1735-1742.

54. R. Chidthong, S. Hannongbua. Excited state properties, fluorescence energies, and lifetimes

of a poly(fluorene-phenylene), based on TD-DFT investigation, *Journal of Computational Chemistry*, **2010**, *31*, 1450-1457.

55. M. Savarese, A. Aliberti, I. De Santo, E. Battista, F. Causa, P. A. Netti, and N. Rega. Fluorescence lifetimes and quantum yields of rhodamine derivatives: New insights from theory and experiment, *Journal of Physical Chemistry A*, **2012**, *116*, 7491-7497.
56. Y. Li and T.-S. Chu. DFT/TDDFT study on the sensing mechanism of a fluorescent probe for hydrogen sulfide: Excited state intramolecular proton transfer coupled twisted intramolecular charge transfer, *Journal of Physical Chemistry A*, **2017**, *121*, 5245-5256.
57. S. Ghosh, K.V.S Girish and S. Ghosh. Evaluation of intramolecular charge transfer state of 4-N, N-dimethylamino cinnamaldehyde using time-dependent density functional theory, *Journal of Chemical Sciences*, **2013**, *125*(4), 933-938.
58. Nguyen Khoa Hien, Mai Van Bay, Phan Diem Tran, Nguyen Tan Khanh, Nguyen Dinh Luyen, Quan V. Vo, Dang Ung Van, Pham Cam Nam and Duong Tuan Quang. A coumarin derivative-Cu2+ complex-based fluorescent chemosensor for detection of biothiols, *RSC Advances*, **2020**, *10, 60*, 36265-36274.
59. P.-F. Loos, A. Scemama, and D. Jacquemin. The quest for highly accurate excitation energies: a computational perspective, *Journal of Physical Chemistry Letters*, **2020**, *11*, 2374-2383.
60. R. E. Stratmann, G. E. Scuseria, M. J. Frisch. An efficient implementation of time-dependent density-functional theory for the calculation of excitation energies of large molecules, *Journal of Chemical Physics*, **1998**, *109*(19), 8218-8224.
61. C. Hu, O. Sugino, K. Watanabe. Performance of Tamm-Dancoff approximation on nonadiabatic couplings by time-dependent density functional theory, *Journal of Chemical Physics*, **2014**, *140*(5), 054106.
62. Mai Van Bay, Nguyen Khoa Hien, Phan Thi Diem Tran, Nguyen Tran Kim Tuyen, Doan Thi Yen Oanh, Pham Cam Nam, Duong Tuan Quang. TD-DFT benchmark for UV-Vis spectra of coumarin derivatives, *Vietnam Journal of Chemistry*, **2021**, *59*(2), 203-210.
63. G. Singh, J. Sindhu, Manisha, V. Kumar, V. Sharma, S. K. Sharma, S. K. Mehta, M. H. Mahnashi, A. Umar and R. Kataria. Development of an off-on selective fluorescent sensor for the detection of Fe3+ ions based on Schiff base and its Hirshfeld surface and DFT studies, *Journal of Molecular Liquids*, **2019**, *296*, 111814.
64. Y. Xia, Z. Qi, Y. Sun, D. Cao, H. Ling, F. Yang, X. Ji. Theoretical investigation of a "turn-on" fluorescent sensor induced by complexation of mercury(II) ion, *Journal of Molecular Modeling*, **2014**, *20*, 2243.
65. S. S. Mallajosyula, H. Usha, A. Datta and S. K. Pati. Molecular modelling of a chemodosimeter for the selective detection of As(III) ion in water, *Journal of Chemical Sciences*, **2008**, *120*(6), 627-635.